Essential and sex-specific effects of mGluR5 in ventromedial hypothalamus regulating estrogen signaling and glucose balance

Micaella P. Fagan[a,1], Dominique Ameroso[a,1], Alice Meng[b], Anna Rock[c], Jamie Maguire[a,c], and Maribel Rios[a,b,c,2]

[a]Graduate Program in Neuroscience, Graduate School of Biomedical Sciences, Tufts University School of Medicine, Boston, MA 02111; [b]Graduate Program in Cell, Molecular and Developmental Biology, Graduate School of Biomedical Sciences, Tufts University School of Medicine, Boston, MA 02111; and [c]Department of Neuroscience, Tufts University School of Medicine, Boston, MA 02111

Edited by Susan G. Amara, NIH, Bethesda, MD, and approved June 30, 2020 (received for review June 3, 2020)

The ventromedial hypothalamus (VMH) plays chief roles regulating energy and glucose homeostasis and is sexually dimorphic. We discovered that expression of metabotropic glutamate receptor subtype 5 (mGluR5) in the VMH is regulated by caloric status in normal mice and reduced in brain-derived neurotrophic factor (BDNF) mutants, which are severely obese and have diminished glucose balance control. These findings led us to investigate whether mGluR5 might act downstream of BDNF to critically regulate VMH neuronal activity and metabolic function. We found that mGluR5 depletion in VMH SF1 neurons did not affect energy balance regulation. However, it significantly impaired insulin sensitivity, glycemic control, lipid metabolism, and sympathetic output in females but not in males. These sex-specific deficits are linked to reductions in intrinsic excitability and firing rate of SF1 neurons. Abnormal excitatory and inhibitory synapse assembly and elevated expression of the GABAergic synthetic enzyme GAD67 also cooperate to decrease and potentiate the synaptic excitatory and inhibitory tone onto mutant SF1 neurons, respectively. Notably, these alterations arise from disrupted functional interactions of mGluR5 with estrogen receptors that switch the normally positive effects of estrogen on SF1 neuronal activity and glucose balance control to paradoxical and detrimental. The collective data inform an essential central mechanism regulating metabolic function in females and underlying the protective effects of estrogen against metabolic disease.

estrogen | glutamate | glucose | ventromedial hypothalamus | synapses

Efficient energy, glucose, and lipid balance control results from coordinated responses of central neural circuits to peripheral signals informing the energy and glycemic status of the animal. Disruptions in these tightly regulated processes can lead to obesity and diabetes. Some of these circuits are located in the VMH, which sensitively responds to caloric signals and sex hormones to regulate energy, glucose, and lipid homeostasis (1–3). These networks include $SF1^+$ neurons, which, in the brain, are exclusive to the VMH and play chief roles in these processes (4, 5).

The VMH is sexually dimorphic, with a higher concentration of estrogen receptors in females compared to males (6). Estrogen receptors within this hypothalamic nucleus, particularly ERα, play paramount roles regulating metabolic function. In support, selective deletion of ERα in $SF1^+$ neurons triggers glucose intolerance and adipocyte hypertrophy in females (7). BDNF and its receptor, TrkB, prominently regulate synaptic plasticity in the mature brain (8) and are also critical components of the neural circuitry controlling energy and glucose homeostasis in the VMH (9–11). Accordingly, whereas selective depletion of BDNF in this nucleus results in obesity, hyperglycemia, insulin resistance, and dyslipidemia (10), global central depletion of this neurotrophin reduces the excitatory drive to VMH neurons (12). In humans, *Bdnf* haploinsufficiency and the functional *Bdnf* Val66Met polymorphism were linked to elevated food intake and body weight (13).

The present study sought to investigate whether identified reductions in the expression of mGluR5 in the VMH of BDNF mutant mice contributed to energy and glucose balance dysregulation. mGluR5 is a part of the group 1 subfamily of metabotropic glutamate receptors, which are expressed near postsynaptic densities and couple with G_q/G_{11} to activate phospholipase-C–mediated signaling via inositol phosphate hydrolysis and subsequent activation of secondary messengers (14). mGluR5 is highly expressed in the VMH and has an integral role regulating excitatory synaptic plasticity in other brain regions (15, 16), but its role in the excitability of VMH cells impacting glycemic and lipid metabolism control has not been studied.

We show that mGluR5 depletion in SF1 neurons in female but not in male mice leads to reduced activity of these cells as well as deficient glucose and lipid balance control. These alterations are due to paradoxical effects of estrogen reducing SF1 neuronal activity and impairing metabolic function in the absence of mGluR5.

Results

mGluR5 Expression Is Reduced in the VMH of BDNF Mutant Mice and Is Regulated by Energy Status. Male and female $BDNF^{2L/2LCk\text{-}cre}$ mice have global central depletion of BDNF and exhibit excessive feeding, glucose intolerance, obesity, and reduced excitatory drive onto VMH neurons (9, 12). Because mGluR5 is highly expressed in the VMH, has an integral role facilitating excitatory synaptic plasticity, and is regulated by BDNF in other brain regions

Significance

Neural circuits in the ventromedial hypothalamus (VMH) play paramount roles mediating glycemic control and lipid metabolism. Work described in this manuscript reveals a sex-specific role of metabotropic glutamate receptor subtype 5 (mGluR5) mediating these effects. It shows that mGluR5 is required in female but not in male VMH to promote activity of $SF1^+$ neurons in this region and glucose and lipid balance control. Importantly, it demonstrates that mGluR5 modulates the effects of estrogen on activity of $SF1^+$ neurons and glycemic control, which switch from faciliatory and protective to deleterious in the absence of this glutamate receptor. The results inform an essential central mechanism regulating metabolic function in females and underlying the protective effects of estrogen against metabolic disease.

Author contributions: M.P.F., D.A., and M.R. designed research; M.P.F., D.A., A.M., A.R., J.M., and M.R. performed research; M.P.F., D.A., A.M., J.M., and M.R. analyzed data; and M.P.F., D.A., and M.R. wrote the paper.

The authors declare no competing interest.

This article is a PNAS Direct Submission.

[1]M.P.F. and D.A. contributed equally to this work.

[2]To whom correspondence may be addressed. Email: maribel.rios@tufts.edu.

This article contains supporting information online at https://www.pnas.org/lookup/suppl/doi:10.1073/pnas.2011228117/-/DCSupplemental.

First published July 27, 2020.

(15–17), we asked whether alterations in its function in the VMH of BDNF$^{2L/2LCk\text{-}cre}$ mutant mice might play a part eliciting these phenotypes. As a first step to test this idea, we measured protein levels of mGluR5 in VMH of BDNF$^{2L/2LCk\text{-}cre}$ mutant and control mice and found that mGluR5 expression levels were significantly decreased in the VMH of female and male mutants (Fig. 1*A*).

We also investigated whether expression of mGluR5 is regulated by energy status in the VMH, as it is the case for BDNF and TrkB (10, 11). We found that mGluR5 protein levels in VMH of fasted wild-type female and male mice were reduced by 41% and 28%, respectively, compared to sex-matched fed mice (Fig. 1*B*). These results suggest that mGluR5 may act downstream of BDNF in the VMH to mediate energy and glucose homeostasis.

mGluR5 in SF1 Neurons Is Not Required for the Regulation of Energy Balance. To directly test the role of mGluR5 in the regulation of metabolic function, we examined the effect of depleting it in SF1^{+} neurons. These cells contain mGluR5 as indicated by RNAscope studies showing colocalization of mGluR5 and SF1 transcripts in the VMH of wild type male and female mice (Fig. 1*C*). Mutant mGluR5$^{2L/2L:SF1\text{-}Cre}$ and control mGluR5$^{2L/2L}$ mice were generated by crossing floxed mGluR5 mice with mice expressing Cre recombinase under the direction of the SF1 promoter. Immunolabeling studies (Fig. 1*D*) and Western blot analysis (Fig. 1 *E* and *F*) show that mGluR5 was depleted in VMH of mGluR5$^{2L/2L:SF1\text{-}Cre}$ mice. Furthermore, mGluR5 depletion did not elicit gross changes in the cytoarchitecture of the VMH (*SI Appendix*, Fig. S1).

Female and male mGluR5$^{2L/2L:SF1\text{-}Cre}$ mice administered a chow diet (Fig. 1 *G–I*) or a high-fat diet (HFD) starting at 8 wk of age (*SI Appendix*, Fig. S2) exhibited normal food intake and body weights compared to controls. Moreover, locomotor activity in female and male mGluR5$^{2L/2L:SF1\text{-}Cre}$ mutants was similar to sex-matched controls (Fig. 1 *J* and *K*). However, there was a significant effect of sex, indicating higher levels of activity in females compared to males. Thermoregulation, measured by core body temperature, was also normal in female and male mutants (Fig. 1*L*). In total, the findings indicate that mGluR5 expression in SF1 neurons is not required for the regulation of energy balance in male or female mice.

mGluR5 Deletion in the VMH Elicits Female-Specific Impairments in Glycemic Control. The VMH is a key glucose-sensing region of the brain facilitating glycemic control (18). Therefore, we investigated whether deleting mGluR5 in SF1 neurons impacted glucose homeostasis in mice fed a chow diet. Fasting levels of glucose were not significantly altered in female mGluR5$^{2L/2L:SF1\text{-}cre}$ mice compared to control females (Fig. 2*A*, time point 0). However, female mutants exhibited impaired responses in the glucose tolerance test (GTT) compared to controls at 8 and 20 wk of age (*SI Appendix*, Fig. S3*A* and Fig. 2 *A* and *B*). In contrast, responses of mGluR5$^{2L/2L:SF1\text{-}cre}$ males (8 and 20 wk of age) to a glucose challenge were indistinguishable from those of male controls (*SI Appendix*, Fig. S3*B* and Fig. 2 *C* and *D*). Accordingly, there was a significant interaction of sex and genotype ($P = 0.02$) in the GTT. Similarly, glucose tolerance was diminished only in mutant females administered an HFD (*SI Appendix*, Fig. S3 *C* and *D*). Finally, mGluR5$^{2L/2L:SF1\text{-}Cre}$ females, but not males, exhibited altered responses in the insulin tolerance test (Fig. 2 *E–H*) and a 140% increase in fasted levels of serum insulin (Fig. 2*I*), indicative of insulin resistance. There was a significant effect of sex on the ITT ($P = 0.03$) and on insulin levels ($P = 0.02$). The collective findings demonstrate a required and sex-specific role of mGluR5 in female SF1 neurons regulating glucose homeostasis.

Female mGluR5$^{2L/2L:SF1\text{-}Cre}$ Mice Exhibit Alterations in Lipid Homeostasis. The VMH is known to influence peripheral lipid metabolism, but the underlying mechanisms are poorly understood (19). We investigated whether mGluR5 in SF1 neurons might influence these functions in mice fed a standard chow diet. Despite exhibiting normal body weights, female but not male mGluR5$^{2L/2L:SF1\text{-}Cre}$ mutants had a 77% increase in triglyceride (TG) content in white adipose tissue (WAT) (Fig. 2*J*). Histological examination of WAT tissue showed that adipocyte hypertrophy accompanied TG accumulation in mutant females (Fig. 2 *K* and *L*) whereas adipocyte size was normal in mutant males (*SI Appendix*, Fig. S4*A*). Finally, liver and serum TG content were not significantly different between genotypes in female or male mice. However, there was a significant effect of sex on serum and liver TG content (*SI Appendix*, Fig. S4 *B* and *C*), with females containing higher levels. The results indicate that mGluR5 plays a requisite role in female VMH regulating lipid metabolism.

mGluR5 Deletion in SF1 Neurons Decreases Sympathetic Outflow in Female Mice. The VMH regulates glucose and lipid metabolism in peripheral tissues via regulation of sympathetic output in the periphery (19–21). We found that norepinephrine levels in serum were significantly reduced in female but not in male mutants (Fig. 2*M*), suggesting decreased sympathetic tone. The results suggest that VMH mGluR5 is required for the regulation of sympathetic output in female but not in male mice.

VMH mGluR5 Is Requisite for Effects of Estradiol Facilitating Glycemic Control. We sought to elucidate mechanisms underlying the observed female-specific effects of depleting mGluR5 in the VMH. Previous studies indicate that mGluR5 functionally interacts with estrogen receptors in other brain regions (22, 23). Therefore, we asked whether mGluR5 is required in the female VMH for effects of estrogen facilitating metabolic function. For this, mGluR5$^{2L/2L}$ and mGluR5$^{2L/2L:SF1\text{-}cre}$ mice were ovariectomized (OVX), and the effects of chronic systemic administration of 17β-estradiol (E2) or vehicle were examined. Both control and mutant OVX mice treated with E2 gained significantly less weight than their vehicle-treated counterparts, indicating that mGluR5 in SF1^{+} neurons is not required for E2-mediated body weight control (Fig. 3*A*).

In far contrast, mGluR5 depletion in SF1 neurons significantly influenced effects of estrogen on glycemic control. Indeed, when data obtained from naïve females (Fig. 2*B*) were included in the analysis, they showed that glucose tolerance was improved in mutant females and no longer different from that of controls following estrogen depletion (Fig. 3 *B* and *C*). Notably, whereas E2 replenishment improved glycemic control in OVX mGluR5$^{2L/2L}$ controls, it produced glucose intolerance in OVX mGluR5$^{2L/2L:SF1\text{-}cre}$ mutants (Fig. 3 *B* and *C*). Accordingly, there was a significant interaction of genotype and treatment in the GTT. The results show that mGluR5 in SF1 neurons is requisite for effects of estradiol facilitating glucose balance in female mice.

Estrogen signals through ERα, ERβ, and GPER1 in mature animals. To further investigate putative mGluR5–ER interactions underlying glycemic control, we asked whether mGluR5 colocalizes with any of these receptors in SF1 neurons of adult females. Fluorescent in situ hybridization (FISH) multiplex analysis indicated a high level of colocalization of mGluR5 with each of these receptors in SF1 neurons in central and dorsomedial VMH (dmVMH; Fig. 3 *D–F* and *SI Appendix*, Table S1). We also examined colocalization in males to determine whether this spatial relationship was sex-specific and found that mGluR5 is also highly coexpressed with estrogen receptors in male SF1 neurons (*SI Appendix*, Table S1).

The high level of colocalization of ERα mRNA with mGluR5 and SF1 transcripts was striking, considering previous reports indicating that ERα expression is limited to the ventrolateral VMH (vlVMH) whereas that of SF1 is limited to central and dmVM in the mature brain (24–26). In contrast, our RNAscope studies indicate that ERα is expressed in adult dmVMH near the

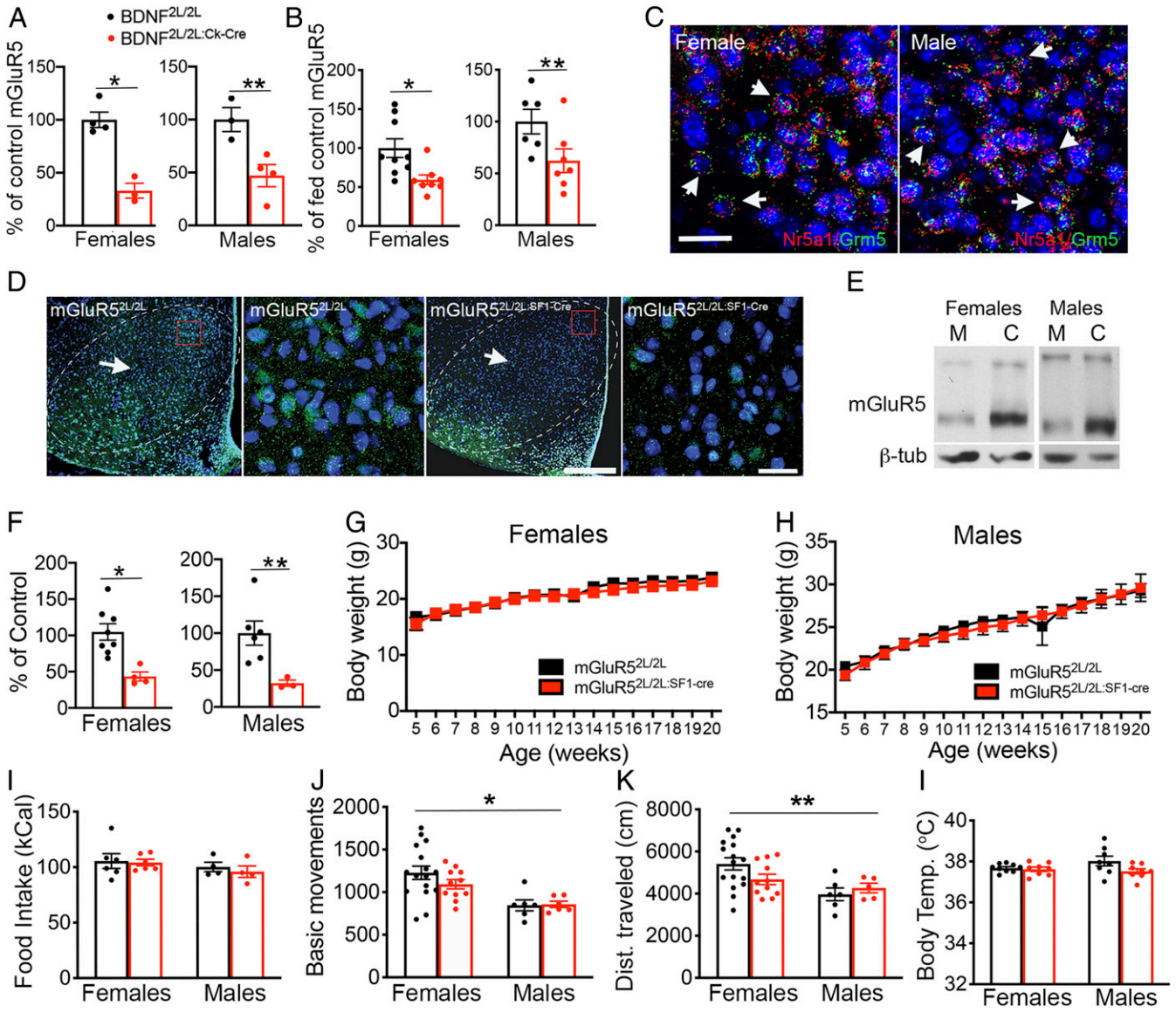

Fig. 1. mGluR5 expression in the VMH is regulated by caloric status and BDNF but is not required for energy balance control. (*A*) mGluR5 protein expression in VMH of female ($n = 4$ controls and $n = 3$ mutants) and male ($n = 3$ controls and $n = 4$ mutants) $BDNF^{2L/2L:Ck\text{-}cre}$ mice and $BDNF^{2L/2L}$ controls. Two-tailed unpaired *t* test: $*P = 0.002$; $**P = 0.02$. (*B*) mGluR5 protein expression in VMH of fed and fasted wild type C57Bl6 male ($n = 6$) and female ($n = 8$) mice. Two-tailed unpaired *t* test: $*P < 0.001$; $**P < 0.05$. (*C*) RNAscope analysis showing expression of mGluR5 transcripts (Grm5; green) in neurons expressing SF1 RNA (Nr5a1; red and arrows) in the wild type female and male VMH. (Scale bar, 25 μM.) (*D*) Low- and high-magnification confocal images from representative sections obtained from $mGluR5^{2L/2L}$ and $mGluR5^{2L/2L:SF1\text{-}cre}$ mice containing VMH (arrows and dashed lines) and immunolabeled with anti-mGluR5 (green) and stained with DAPI (blue). Red boxes in low-magnification images represent areas shown in the high-magnification images. (Scale bars: low magnification, 250 μM; high magnification, 20 μM.) (*E*) Representative Western blot showing mGluR5 protein content in $mGluR5^{2L/2L:SF1\text{-}cre}$ mutants and $mGluR5^{2L/2L}$ controls. (*F*) mGluR5 protein content in female ($n = 8$ controls and $n = 4$ mutants) and male ($n = 6$ controls and $n = 3$ mutants) $mGluR5^{2L/2L:SF1\text{-}cre}$ and $mGluR5^{2L/2L}$ mice. Two-tailed unpaired *t* test: $*P = 0.005$; $**P = 0.03$. (*G*) Body weights of female ($n = 6$) $mGluR5^{2L/2L:SF1\text{-}cre}$ and $mGluR5^{2L/2L}$ controls. (*H*) Body weights of male $mGluR5^{2L/2L:SF1\text{-}cre}$ ($n = 5$) and $mGluR5^{2L/2L}$ controls ($n = 8$). (*I*) Weekly food intake (chow) of female ($n = 6$) and male ($n = 5$) $mGluR5^{2L/2L:SF1\text{-}cre}$ and $mGluR5^{2L/2L}$ controls. (*J* and *K*) Locomotor activity of female ($n = 11$) and male ($n = 6$) $mGluR5^{2L/2L:SF1\text{-}cre}$ mutants and $mGluR5^{2L/2L}$ controls. Two-way ANOVA: sex, $*P = 0.0007$; $**P = 0.01$. (*L*) Core body temperature in female ($n = 8$) and male ($n = 8$) $mGluR5^{2L/2L:SF1\text{-}cre}$ mutants and $mGluR5^{2L/2L}$ controls. Data are presented as means ± SEM.

third ventricle, albeit at lower levels that in the vlVMH (*SI Appendix*, Fig. S5*A*). Moreover, cells with lower SF1 expression relative to dmVMH were observed in vlVMH. Colocalization analysis indicates that 70.8% and 69.4% of SF1 neurons of adult females in the dmVMH and vlVMH, respectively, contain ERα, whereas 94.5% and 65.8% of $ERα^+$ cells in the dmVMH and vlVMH, respectively, contain SF1 (*SI Appendix*, Table S2). The conflicting evidence might emerge from differences in the sensitivity of detection methods used for identifying SF1 and ERα-containing cells in each of the studies. Indeed, a single transcript per cell can be detected using RNAscope technology (27). Consistent with our findings, studies from the Allen Brain Institute (ABI) show ERα transcripts in the dmVMH and $SF1^+$ cells in the vlVMH (*SI Appendix*, Fig. S5*B*) (28, 29). The specificity of the SF1 probes used in the ABI and our RNAscope studies (*SI Appendix*, Fig. S5 *B* and *C*) is indicated by the lack of signal in hippocampus and cortex, consistent with $SF1^+$ cells being exclusive to the VMH in the adult brain. The collective

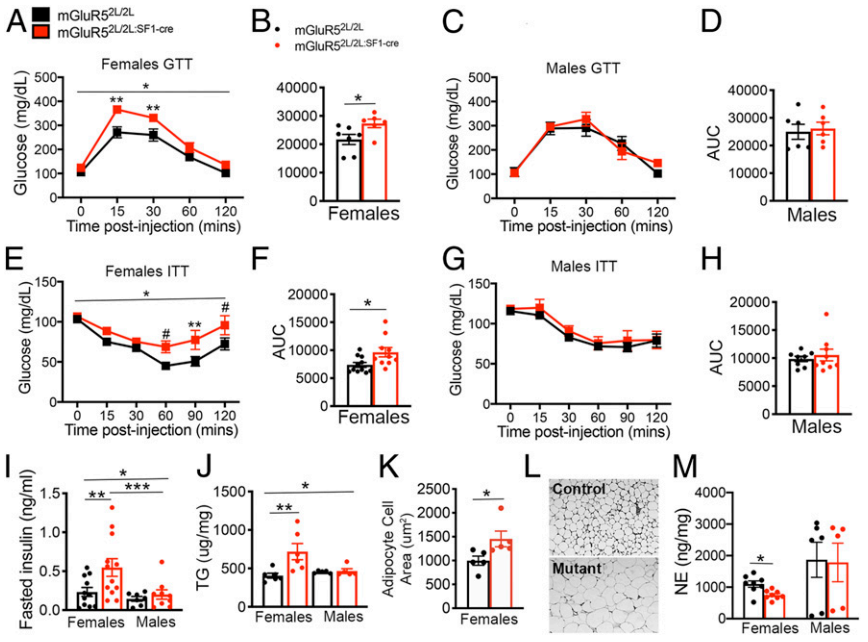

Fig. 2. mGluR5 is required in female but not in male SF1 neurons for the regulation of glucose and lipid balance and sympathetic output. (*A*) Glucose tolerance test (GTT) in mGluR5$^{2L/2L:SF1\text{-}cre}$ (n = 6) and mGluR5$^{2L/2L}$ (n = 7) females. *Two-way ANOVA: genotype, P = 0.02; time, P < 0.0001; interaction, P = 0.006. Bonferroni's multiple comparisons test: **P < 0.05. (*B*) Area under the curve (AUC) for the GTT in females. Two-tailed unpaired t test: *P = 0.04. (*C*) Glucose tolerance test (GTT) in mGluR5$^{2L/2L:SF1\text{-}cre}$ (n = 6) and mGluR5$^{2L/2L}$ (n = 6) males. (*D*) AUC for the GTT in males. (*E*) Insulin tolerance test (ITT) in mGluR5$^{2L/2L:SF1\text{-}cre}$ (n = 10) and mGluR5$^{2L/2L}$ (n = 11) females. *Two-way ANOVA: genotype, P = 0.02. Bonferroni's multiple comparisons test: $^{\#}P$ = 0.08; **P = 0.03. (*F*) AUC for the ITT in females. Two-tailed unpaired t test: *P = 0.02. (*G*) ITT in mGluR5$^{2L/2L:SF1\text{-}cre}$ (n = 9) and mGluR5$^{2L/2L}$ (n = 8) males. (*H*) AUC for the ITT in males. (*I*) Serum levels of insulin in fasted control (n = 11) and mutant (n = 12) females and control (n = 7) and mutant (n = 9) males. *Two-way ANOVA: genotype, P = 0.04; sex, P = 0.02. Bonferroni's multiple comparisons test: **P = 0.04; ***P = 0.03. (*J*) Triglyceride (TG) levels in WAT of control and mutant females (n = 6) and control and mutant males (n = 5). *Two-way ANOVA: genotype, P = 0.02; interaction of sex and genotype, P = 0.03. Bonferroni's multiple comparisons test: **P = 0.01. (*K*) Adipocyte cell area in mGluR5$^{2L/2L:SF1\text{-}cre}$ and mGluR5$^{2L/2L}$ (n = 5) females. Two-tailed unpaired t test: *P < 0.04. (*L*) Representative images of WAT in control and mutant females. (*M*) Serum levels of norepinephrine (NE) in control and mutant females (n = 8) and control (n = 6) and mutant males (n = 5). Two-tailed unpaired t test: *P < 0.01. Data are presented as means ± SEM.

data indicate that SF1 neurons in the adult VMH contain ERα, ERβ, and GPER1 and are sensitive to estrogen. Therefore, it is possible that mGluR5 interacts with estrogen receptors in SF1 neurons to facilitate glycemic control in adulthood.

We sought to identify estrogen receptors mediating aberrant responses to estrogen in mutant females. Effects of estrogen facilitating glucose homeostasis have been attributed primarily to ERα (7, 30). We found that naïve mGluR5$^{2L/2L:SF1\text{-}cre}$ females had a 30% decrease in ERα protein content in the VMH, whereas mGluR5$^{2L/2L:SF1\text{-}cre}$ males had increased expression compared to sex-matched controls (Fig. 4*A*). Protein levels of ERβ and GPER1 in VMH were normal in all mutants (Fig. 4 *B* and *C*). Responses to selective ERα, ERβ, or GPER1 receptor activation were also examined. Whereas chronic systemic delivery of the selective ERα agonist propyl pyrazole triol (PPT) significantly mitigated glucose intolerance in OVX mGluR5$^{2L/2L}$ controls, its effects were significantly diminished in OVX mGluR5$^{2L/2L:SF1\text{-}cre}$ mutants. Accordingly, there was a significant interaction of genotype and treatment in the GTT and AUC (Fig. 4 *D* and *E*).

Glucose balance control is normal in ERβ-deficient female and male mice, negating an essential role in the underlying regulatory mechanisms (31). However, it has been proposed that ERβ antagonizes the beneficial metabolic effects of ERα (32). We found that delivery of the ERβ-selective agonist diarylpropionitrile (DPN) mildly compromised glucose tolerance in controls and mutants (Fig. 4 *F* and *G*). Finally, we examined the effects of chronic delivery of G1 to assess GPER1 function. Whereas G1 diminished glucose tolerance in mGluR5$^{2L/2L:SF1\text{-}cre}$ females, it had no effect in mGluR5$^{2L/2L}$controls. Accordingly, there was a significant interaction of treatment and genotype in the GTT and in AUC (Fig. 4 *H* and *I*). Body weights of mGluR5$^{2L/2L:SF1\text{-}cre}$ and mGluR5$^{2L/2L}$ females treated with PPT, DPN, and G1 were not significantly different (*SI Appendix*, Fig. S6), indicating that abnormal responses of mutant females were not related to alterations in body weight.

In total, the findings show that VMH mGluR5 is critical for estradiol's protective influence on glucose balance control and responses to selective ER activation. Notably, the data suggest that, in the absence of mGluR5, deficits in ERα function compounded by a detrimental gain of GPER1 function leads to paradoxical responses to estrogen in females, impeding glycemic control.

Firing Rate of SF1 Neurons Is Significantly Reduced in Female but Intact in Male mGluR5$^{2L/2L:SF1\text{-}Cre}$ Mice. To inform neurobiological mechanisms underlying the metabolic alterations of mGluR5$^{2L/2L:SF1\text{-}cre}$ females and their altered responses to estradiol, we conducted an electrophysiological examination of SF1 neurons located in central and dorsomedial VMH. Whole-cell recordings were performed in mGluR5$^{2L/2L:SF1\text{-}cre}$ mutants and controls with selective expression of the tdTomato reporter in SF1 neurons. Firing rate of SF1 neurons in mGluR5$^{2L/2L:SF1\text{-}cre}$ males was normal compared to sex-matched controls (Fig. 5 *A* and *E*), consistent with their normal metabolic profile.

In addition to examining naïve females, we asked whether aberrant responses to E2 delivery in the GTT exhibited by OVX mGluR5$^{2L/2L:SF1\text{-}cre}$ mutants might be related to abnormal responses of SF1 neurons to estrogen. To fully capture the total effect of estrogen acting through all receptors, we performed these experiments in OVX mice with systemic chronic delivery of E2 or vehicle. mGluR5$^{2L/2L:SF1\text{-}cre}$ mutants exhibited reduced neuronal activity compared to mGluR5$^{2L/2L}$ controls only when estradiol was present. Accordingly, there was a significant effect of genotype and a significant interaction of treatment and genotype (Fig. 5 *B–D* and *F*). Levels of estradiol influenced the activity of SF1 neurons in control females, indicating an adult function of this hormone regulating this cell population. Accordingly, SF1 neuronal firing in mGluR5$^{2L/2L}$ females was reduced by estrogen depletion and restored to levels of naïve controls following E2 replacement (Fig. 5*F*). The collective data indicate that mGluR5 in the adult brain promotes activity of SF1 neurons and is required for effects of estradiol increasing the activity of these cells in female mice.

Intrinsic Excitability of SF1 Neurons Is Reduced in mGluR5$^{2L/2L:SF1\text{-}cre}$ Females. We measured the intrinsic excitability of SF1 neurons to inform mechanisms underlying the reduced activity of these cells in mutant females. The response to increasing depolarizing

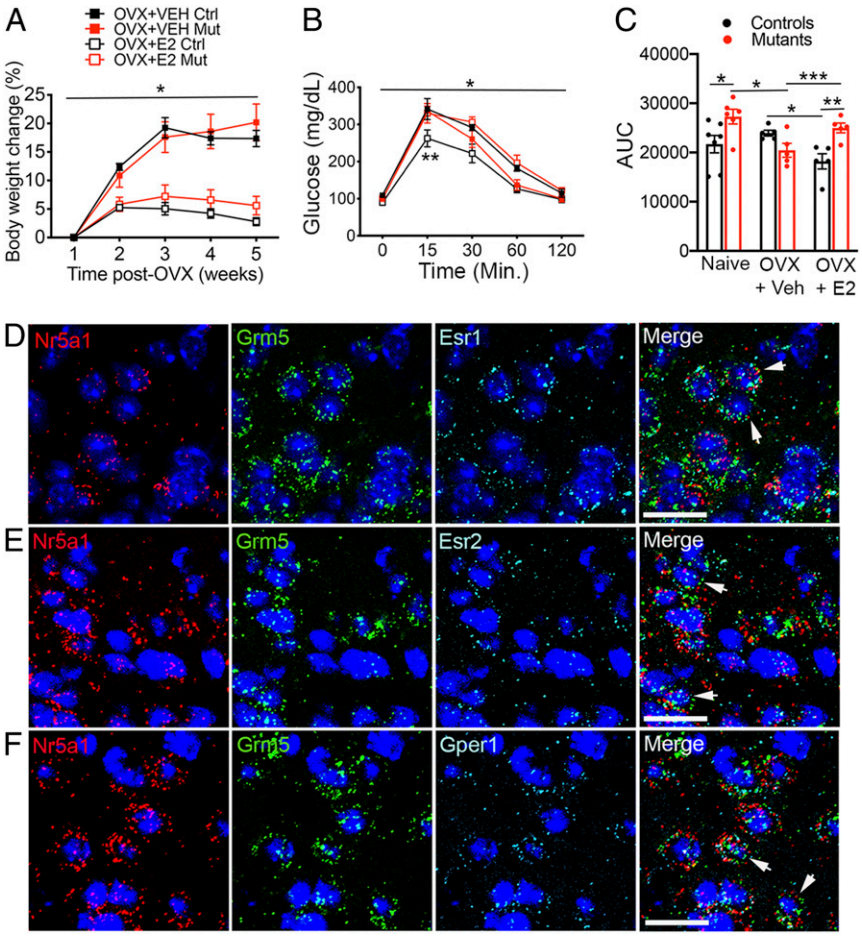

Fig. 3. Aberrant effects of estrogen on glycemic control in female mice depleted of mGluR5 in SF1 neurons. (*A*) Body weights of OVX mGluR5$^{2L/2L}$ (Ctrl) and mGluR5$^{2L/2L:SF1\text{-}cre}$ (Mut) mice treated with vehicle (VEH) or 17β-estradiol (E2; $n = 5$ for all groups). *Two-way ANOVA: treatment, $P < 0.0001$. (*B*) GTT in OVX mGluR5$^{2L/2L}$ and mGluR5$^{2L/2L:SF1\text{-}cre}$ mice treated with vehicle or 17β-estradiol ($n = 5$ for all groups). *Three-way ANOVA: genotype, $P = 0.03$; interaction of treatment and genotype, $P < 0.0001$; time, $P < 0.0001$, $^{**}P < 0.05$. (*C*) Area under the curve (AUC) for the GTT in naïve mGluR5$^{2L/2L}$ ($n = 7$) and mGluR5$^{2L/2L:SF1\text{-}cre}$ ($n = 6$) females and OVX mice ($n = 5$ for all groups). Two-way ANOVA: treatment, $P = 0.02$; genotype, $P = 0.1$; interaction, $P = 0.003$. Bonferroni's multiple comparisons test: $^{*}P = 0.007$; $^{**}P = 0.002$; $^{***}P = 0.03$. Multiplex RNAscope analysis of SF1 and mGluR5 transcript colocalization (arrows) with ERα (*D*), ERβ (*E*), or GPER1 (*F*) RNA in VMH of wild type females. (Scale bar, 25 μM.) Data are presented as means ± SEM.

current and the resting membrane potential was normal in mGluR5$^{2L/2L:SF1\text{-}cre}$ males (Fig. 5 *G* and *H*). In contrast, mutant females exhibited decreased responses and normal resting membrane potential (Fig. 5 *I* and *J*). Accordingly, there was a significant interaction of sex and genotype ($P < 0.0001$), indicating that mGluR5 critically regulates the intrinsic excitability of SF1 neurons is female but not in male mice.

Next, we asked whether levels of VMH activity following a glucose challenge were altered to inform mechanisms underlying diminished glycemic control in mutant females. For this, we measured density of c-fos^{+} cells in the VMH as a surrogate for neuronal activity at 30 min post glucose administration in females fasted for 16 h. Glucose-treated mutant females exhibited a 76% decrease in c-fos^{+} cells compared to controls, indicating diminished neuronal activity (Fig. 5*K* and *SI Appendix*, Fig. S7).

Depletion of mGluR5 in Females but Not in Males Impairs Excitatory Synaptic Transmission in the VMH. We investigated whether mGluR5 might control activity of SF1 neurons via regulation of the synaptic excitatory drive onto these cells. SF1 neurons in mutant males exhibited normal frequency and amplitude of spontaneous excitatory postsynaptic currents (sEPSCs; Fig. 6 *A* and *B*). In contrast, there was a significant interaction of treatment and genotype on sEPSC frequency in females (Fig. 6 *D* and *E*), indicating that estrogen decreased the excitatory tone onto mutant SF1 neurons. Accordingly, whereas there was a trend toward reduced sEPSC frequency in naïve mutants compared to naïve controls, this difference was no longer evident following estrogen depletion (OVX + vehicle; Fig. 6*D*). This effect was mostly driven by an increase in frequency of sEPSCs in mGluR5$^{2L/2L:SF1\text{-}cre}$ mice following ovariectomy (Fig. 6*D*). No differences in amplitude of EPSCs were observed (Fig. 6*E*). Finally, a significant interaction of sex and genotype ($P = 0.03$) indicated that the effect of mGluR5 depletion on excitatory drive onto SF1 neurons was female-specific.

We measured the density of presynaptic vGlut2^{+} puncta onto SF1^{+} neurons to determine whether altered content of excitatory synapses underlies the reduced excitatory tone in mGluR5$^{2L/2L:SF1\text{-}cre}$ females. Consistent with the electrophysiological studies, we found that excitatory synapse content was significantly reduced in mGluR5$^{2L/2L:SF1\text{-}cre}$ females compared to controls when estrogen was present. Accordingly, naïve mutant females exhibited a 42% reduction in the number of excitatory synapses onto SF1^{+} cells compared to naïve controls (Fig. 6 *F* and *G*). This deficit was not observed following estrogen depletion but reemerged when E2 was replenished in OVX mice (Fig. 6 *F* and *G*). Finally, NMDA and AMPA1 receptor content in VMH of naïve mGluR5$^{2L/2L:SF1\text{-}cre}$ females was also assessed and found to be normal (*SI Appendix*, Fig. S8*A*).

In total, the data indicate that mGluR5 depletion reduces the excitatory tone onto SF1^{+} neurons exclusively in females and that this deficit is associated with reduced density of excitatory synapses in the VMH. Moreover, they indicate that estrogen paradoxically reduces the excitatory drive onto SF1 neurons in the absence of mGluR5.

Depletion of mGluR5 Potentiates Inhibitory Synaptic Transmission in SF1 Neurons in Females but Not in Males. We investigated the effects of depleting mGluR5 on inhibitory transmission in the VMH. Frequency and amplitude of spontaneous inhibitory postsynaptic currents (sIPSCs) were normal in SF1 neurons of

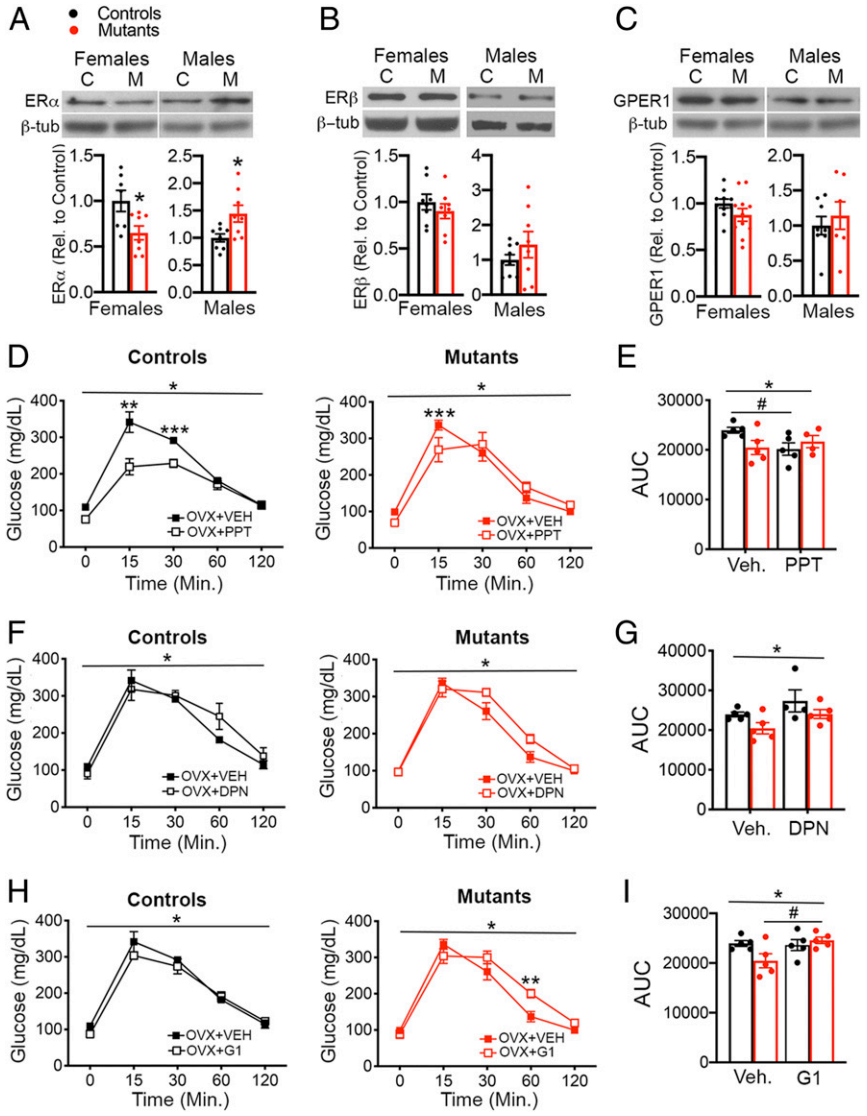

Fig. 4. Selective estrogen receptor stimulation elicits abnormal responses of OVX mGluR5$^{2L/2L:SF1\text{-}cre}$ females in the GTT. (*A*) ERα protein content in VMH of mGluR5$^{2L/2L}$ and mGluR5$^{2L/2L:SF1\text{-}cre}$ females ($n = 7$ for each group) and males ($n = 8$ for each group). Two-tailed unpaired *t* test: $^{*}P = 0.02$ for females and males. (*B*) ERβ protein content in VMH of mGluR5$^{2L/2L}$ and mGluR5$^{2L/2L:SF1\text{-}cre}$ females ($n = 8$ for each group) and males ($n = 8$ for each group). (*C*) GPER1 protein content in VMH of mGluR5$^{2L/2L}$ and mGluR5$^{2L/2L:SF1\text{-}cre}$ females ($n = 10$ for each group) and males ($n = 8$ for each group). (*D*) GTT in OVX mGluR5$^{2L/2L}$and mGluR5$^{2L/2L:SF1\text{-}cre}$ females treated with vehicle ($n = 5$; same vehicle-treated groups as those used in E2-delivery experiments) or the selective ERα agonist PPT ($n = 5$ for controls and $n = 4$ for mutants). Three-way ANOVA: treatment, $P = 0.0006$; interaction of treatment and genotype, $P = 0.005$; time, $P < 0.0001$. Bonferroni's multiple comparisons test for PPT GTT: $^{**}P < 0.001$; $^{***}P = 0.03$. (*E*) AUC for the GTT in OVX mGluR5$^{2L/2L}$and mGluR5$^{2L/2L:SF1\text{-}cre}$ females treated with vehicle or the selective ERα agonist (Ago) PPT. *Two-way ANOVA: interaction of treatment and genotype, $P = 0.05$. Bonferroni's multiple comparisons test for PPT: $^{\#}P = 0.06$. (*F*) GTT in OVX mGluR5$^{2L/2L}$ and mGluR5$^{2L/2L:SF1\text{-}cre}$ females treated with vehicle ($n = 5$; same vehicle-treated groups as those used in E2-delivery experiments) or the selective ERβ agonist DPN ($n = 4$ for controls and $n = 5$ for mutants. *Three-way ANOVA: treatment, $P = 0.06$; genotype, $P = 0.02$; time, $P < 0.0001$. (*G*) AUC for the GTT in OVX mGluR5$^{2L/2L}$and mGluR5$^{2L/2L:SF1\text{-}cre}$ females treated with vehicle or DPN. *Two-way ANOVA: treatment, $P = 0.04$; genotype, $P = 0.04$. (*H*) GTT in OVX mGluR5$^{2L/2L}$and mGluR5$^{2L/2L:SF1\text{-}cre}$ females treated with vehicle ($n = 5$; same vehicle-treated groups as those used in E2-delivery experiments) or the selective GPER1 agonist G1 ($n = 5$ for controls and mutants). *Three-way ANOVA: interaction of treatment and genotype, $P = 0.03$; time, $P < 0.001$. Bonferroni's multiple comparisons test: $^{**}P = 0.01$. (*I*) AUC for the GTT in OVX mGluR5$^{2L/2L}$and mGluR5$^{2L/2L:SF1\text{-}cre}$ females treated with vehicle or G1. *Two-way ANOVA: interaction of treatment and genotype, $P = 0.04$. Bonferroni's multiple comparisons test for G1: $^{\#}P = 0.06$. GTT data for controls and mutants were analyzed together but presented separately by genotype for clarity. Data presented as means ± SEM.

mGluR5$^{2L/2L:SF1\text{-}cre}$ males (Fig. 7 *A* and *B*). In contrast, inhibitory tone was elevated in mutant females, and this alteration was driven, at least in part, by estrogen. In support, frequency of sIPSCs was significantly increased in naïve mGluR5$^{2L/2L:SF1\text{-}cre}$ females compared to naïve controls (Fig. 7 *C* and *D*). This alteration was no longer evident following depletion of estrogen, which reduced the frequency of sIPSCs in mutants compared to their naïve counterparts (Fig. 7 *C* and *D*). However, the elevated inhibitory drive onto mutant SF1 neurons was apparent again following E2 replenishment, which significantly increased the frequency of sIPSCs in OVX mutants compared to vehicle-treated mutants (Fig. 7 *C*–*E*). Finally, a significant interaction of sex and genotype in frequency ($P = 0.008$) and a trend for amplitude ($P = 0.08$) of sIPSCs indicated that the effect of mGluR5 depletion elevating the inhibitory tone of SF1 neurons was female-specific.

Expression levels of $GABA_A$ receptors in the VMH were measured to ascertain mechanisms underlying the increased inhibitory drive observed in female SF1 neurons lacking mGluR5. Levels of synaptic $GABA_A$ γ2 were similar in naïve control and mutant females (*SI Appendix*, Fig. S8*B*). Content of the GABAergic synthetic enzymes glutamic acid decarboxylase (GAD) 65 and 67 in the VMH was also measured, as they influence GABAergic tone (33, 34). Whereas expression of GAD65 was normal, GAD67 protein content was significantly increased in the VMH of naïve mutant females (Fig. 7*F*). E2 administration differentially affected inhibitory transmission in OVX mGluR5$^{2L/2L:SF1\text{-}cre}$ females compared to OVX mGluR5$^{2L/2L}$ controls (Fig. 7 *D* and *E*). Thus, we posited that differences in the regulation of GAD67 by E2 might be responsible. Whereas GAD67 expression was not significantly different in OVX mGluR5$^{2L/2L}$ and mGluR5$^{2L/2L:SF1\text{-}cre}$ treated with vehicle, there was a trend toward a significant elevation in mutants compared to controls following E2 treatment (Fig. 7*G*).

The possibility that alterations in inhibitory synapse density contributed to the hyperinhibition of SF1 neurons in mutant females was also investigated. Estrogen levels influenced the inhibitory synaptic organization in the VMH of both control and mutant females. Naïve mGluR5$^{2L/2L:SF1\text{-}cre}$ females displayed a 63% increase in vGAT^{+} inputs onto SF1 neurons compared to naïve mGluR5$^{2L/2L}$ controls (Fig. 7 *H* and *I*). Notably, estrogen depletion had opposite effects in controls and mutants, increasing and decreasing their number of inhibitory synapses, respectively. Accordingly, mGluR5$^{2L/2L}$ mice contained 92% more vGAT^{+} puncta compared to mutants following ovariectomy and vehicle delivery (Fig. 7 *H* and *I*). Finally, E2 delivery in OVX mice reduced the number of vGAT^{+} puncta in mGluR5$^{2L/2L}$ controls but not in mGluR5$^{2L/2L:SF1\text{-}cre}$ females compared to vehicle treatment (Fig. 7 *H* and *I*).

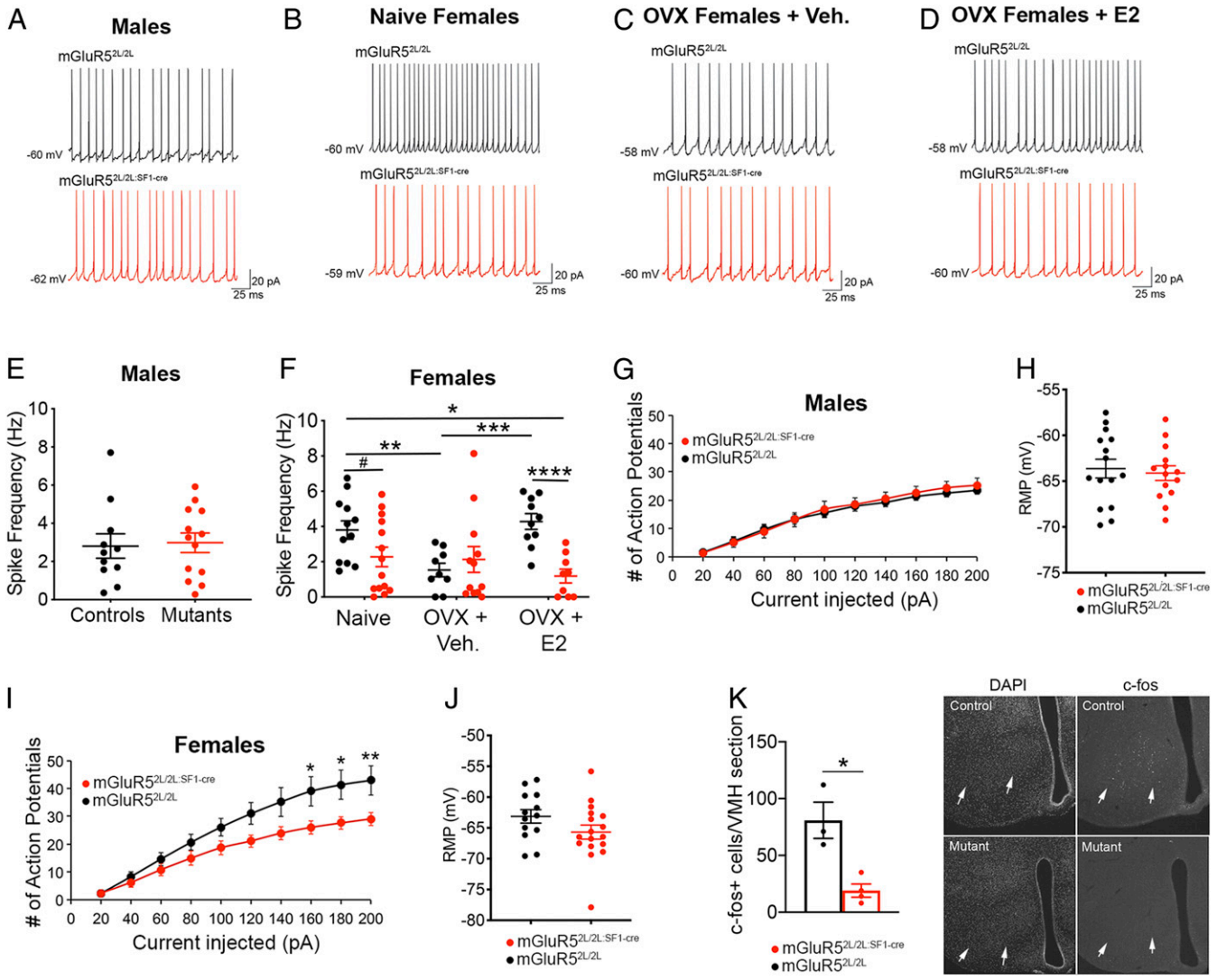

Fig. 5. mGluR5 critically regulates the firing rate and intrinsic excitability of SF1 neurons in females, but not in males, and activity responses of these cells to estradiol. Representative traces of SF1 neurons at resting membrane potential from mGluR5$^{2L/2L}$ and mGluR5$^{2L/2L:SF1\text{-}cre}$ males (*A*) and naïve (*B*), OVX + vehicle (*C*), and OVX + E2 (*D*) mGluR5$^{2L/2L}$ and mGluR5$^{2L/2L:SF1\text{-}cre}$ females. (*E*) Spike frequency of SF1 neurons in mGluR5$^{2L/2L}$ (n = 12 cells, n = 4 animals) and mGluR5$^{2L/2L:SF1\text{-}cre}$ (n = 13 cells, n = 5 animals) males. (*F*) Spike frequency of SF1 neurons in naïve mGluR5$^{2L/2L}$ (n = 12 cells, n = 4 animals) and mGluR5$^{2L/2L:SF1\text{-}cre}$ (n = 14 cells, n = 4 animals) females, OVX mGluR5$^{2L/2L}$ (n = 9 cells, n = 3 animals) and mGluR5$^{2L/2L:SF1\text{-}cre}$ (n = 12 cells, n = 4 animals) females treated with vehicle, and OVX mGluR5$^{2L/2L}$ (n = 10 cells, n = 4 animals) and mGluR5$^{2L/2L:SF1\text{-}cre}$ (n = 9 cells, n = 3 animals) E2-treated females. *Two-way ANOVA: genotype, P = 0.005; interaction of genotype and treatment, P = 0.01. Bonferroni's multiple comparisons test: **P = 0.02; ***P = 0.006; ****P = 0.002; $^{\#}P$ = 0.1. (*G*) Neuronal firing rate (Hz) of SF1 neurons in response to increasing 20-pA current injection (pA) steps and in mGluR5$^{2L/2L:SF1\text{-}cre}$ (n = 14 cells, n = 4 animals) and mGluR5$^{2L/2L:SF1\text{-}cre}$ (n = 14 cells, n = 5 animals) males. (*H*) Resting membrane potential of SF1 neurons in mGluR5$^{2L/2L:SF1\text{-}cre}$ (n = 14 cells, n = 4 animals) and mGluR5$^{2L/2L:SF1\text{-}cre}$ (n = 14 cells, n = 5 animals) males. (*I*) Neuronal firing rate (Hz) of SF1 neurons in response to increasing 20-pA current injection (pA) steps and in mGluR5$^{2L/2L:SF1\text{-}cre}$ (n = 13 cells, n = 4 animals) and mGluR5$^{2L/2L:SF1\text{-}cre}$ (n = 15 cells, n = 4 animals) females. Two-way ANOVA: genotype, $P < 0.0001$. Bonferroni's multiple comparisons test: *$P < 0.05$; **$P < 0.01$. (*J*) Resting membrane potential of SF1 neurons in mGluR5$^{2L/2L:SF1\text{-}cre}$ (n = 13 cells, n = 4 animals) and mGluR5$^{2L/2L:SF1\text{-}cre}$ (n = 15 cells, n = 4 animals) males. (*K*) c-fos^{+} cells in VMH (arrows) of fasted mGluR5$^{2L/2L:SF1\text{-}cre}$ (n = 3) and mGluR5$^{2L/2L:SF1\text{-}cre}$ (n = 4) females 30 min following injection of a bolus of glucose. *P = 0.01, unpaired t test. Data presented as means ± SEM.

The collective data indicate that mGluR5 critically regulates the inhibitory tone in the adult VMH via regulation of GAD67 expression and density of inhibitory synapses onto SF1 neurons. Notably, they show that effects of estrogen become paradoxical in the absence of mGluR5, leading to a significant increase in the inhibitory drive onto SF1 neurons.

Discussion

Here we demonstrate an essential and sex-specific role of mGluR5 in the VMH facilitating sympathetic output and glucose and lipid balance in female mice. Effects of mGluR5 on firing rate, intrinsic excitability, and excitatory and inhibitory synaptic transmission in SF1 neurons underlie these sex-specific actions. Importantly, the studies show that mGluR5 greatly influences the effects of estradiol on activity of SF1 neurons and glycemic control, which switch from faciliatory to deleterious in the absence of this glutamate receptor. The collective data inform an essential central mechanism regulating metabolic function and underlying the protective effects of estrogen against metabolic disease.

We found that VMH mGluR5 is not required for the regulation of energy balance in females or males. This is in contrast with BDNF$^{2L/2L:Ck\text{-}cre}$ mutant mice, which are profoundly hyperphagic

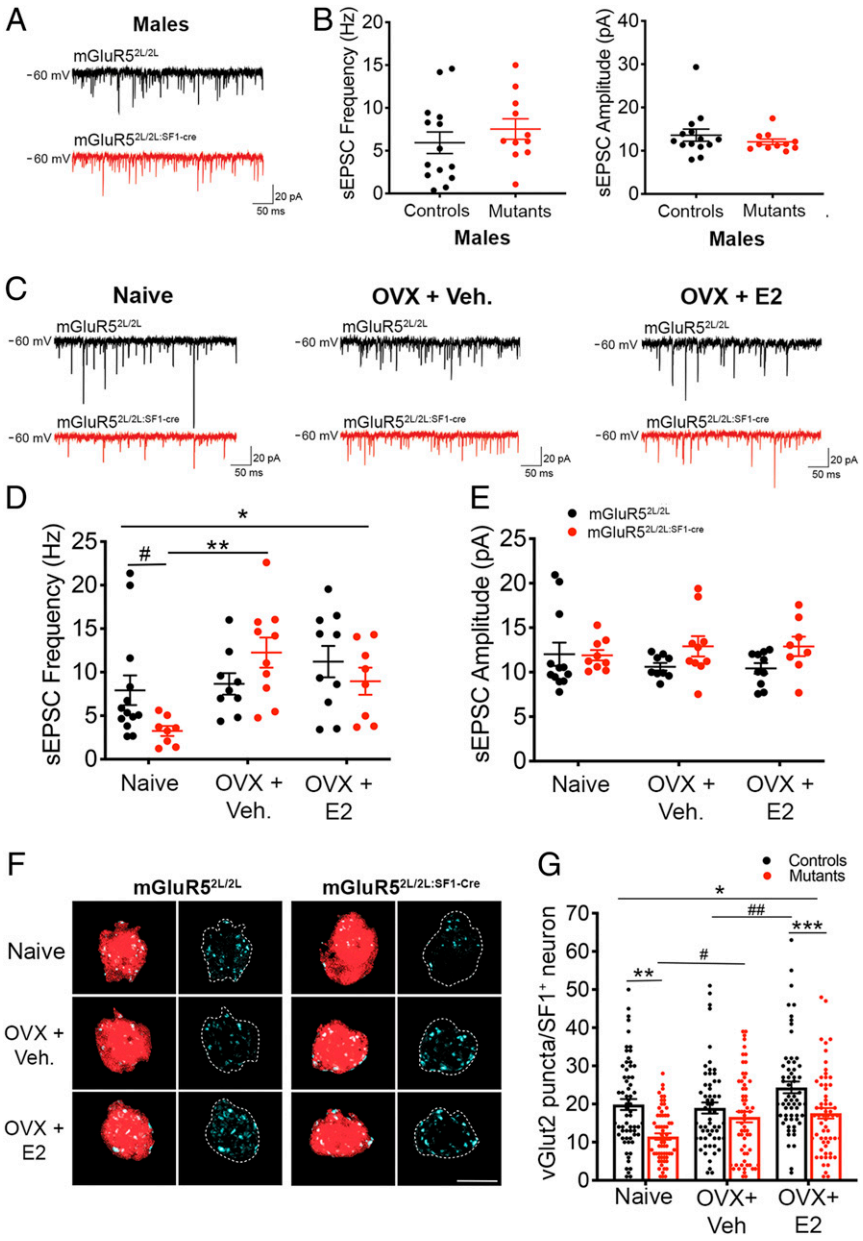

Fig. 6. mGluR5 depletion diminishes the excitatory tone and alters synaptic responses of SF1 neurons to estrogen in females. (*A*) Representative sEPSC traces from SF1 neurons held at −60 mV from mGluR5$^{2L/2L}$ and mGluR5$^{2L/2L:SF1\text{-}cre}$ males. (*B*) sEPSC frequency (Hz) and amplitude (pA) in SF1 neurons from mGluR5$^{2L/2L}$ (n = 14 cells, n = 6 animals) and mGluR5$^{2L/2L:SF1\text{-}cre}$ (n = 11 cells, n = 3 animals) males. Student's t test: NS. (*C*) Representative sEPSC traces from SF1 neurons from naïve, OVX + vehicle, and OVX + E2 mGluR5$^{2L/2L}$ and mGluR5$^{2L/2L:SF1\text{-}cre}$ females. (*D*) sEPSC frequency (Hz) in SF1 neurons of naïve mGluR5$^{2L/2L}$ (n = 13 cells, n = 4 animals) and mGluR5$^{2L/2L:SF1\text{-}cre}$ (n = 8 cells, n = 4 animals) females, OVX mGluR5$^{2L/2L}$ (n = 9 cells, n = 3 animals) and mGluR5$^{2L/2L:SF1\text{-}cre}$ (n = 10 cells, n = 4 animals) females treated with vehicle, and OVX mGluR5$^{2L/2L}$ (n = 10 cells, n = 3 animals) and mGluR5$^{2L/2L:SF1\text{-}cre}$ (n = 8 cells, n = 4 animals) females treated with E2. *Two-way ANOVA: treatment, $P = 0.005$; interaction of genotype and treatment, $P = 0.03$. Bonferroni's multiple comparisons test: $^{**}P = 0.001$; $^{\#}P = 0.09$. (*E*) sEPSC amplitude (pA) of SF1 neurons in naïve, OVX + vehicle, and OVX + E2 mGluR5$^{2L/2L}$ and mGluR5$^{2L/2\text{-}L:SF1\text{-}cre}$ females. (*F*) Representative immunolabeling of presynaptic vGlut2^{+} (cyan) puncta onto SF1^{+} cells within the VMH of naïve, OVX + vehicle, and OVX + E2 mGluR5$^{2L/2L}$ and mGluR5$^{2L/2L:SF1\text{-}cre}$ females. (*G*) Quantification of vGlut2^{+} puncta onto SF1 neurons of mGluR5$^{2L/2L}$ and mGluR5$^{2L/2L:SF1\text{-}cre}$ females (n = 3 mice and n = 18 to 20 cells per animal). *Two-way ANOVA: genotype, $P < 0.0001$; treatment, $P = 0.0005$; interaction of genotype and treatment, $P = 0.07$. Bonferroni's multiple comparisons test: $^{**}P = 0.0002$; $^{***}P = 0.006$; $^{\#}P = 0.08$; $^{\#\#}P = 0.06$. All data presented as means ± SEM.

and obese, in addition to exhibiting reduced VMH mGluR5 expression (9). The findings suggest that BDNF acts through mGluR5-independent mechanisms or that SF1^{+} cells are not a critical substrate for mGluR5 in the VMH to achieve energy homeostasis. Despite having normal body weights, mGluR5$^{2L/2L:SF1\text{-}cre}$ females, but not males, displayed insulin resistance and deficits in glucose tolerance, indicating a sex-specific role of VMH mGluR5 facilitating glucose metabolism. Female mutants also had an elevated content of triglycerides in WAT, indicating aberrant lipid metabolism. The decreased sympathetic output observed exclusively in female mGluR5$^{2L/2L:SF1\text{-}cre}$ mutants might underlie these perturbations. In support, SF1^{+} fibers are located in close apposition to cell bodies in the nucleus of the solitary tract and rostroventrolateral medulla, which are autonomic centers in the brainstem regulating sympathetic outflow (20). Furthermore, electrical stimulation of the VMH increases glucose uptake in skeletal muscle, and this effect is blunted by sympathetic denervation (35, 36). Finally, stimulation of sympathetic fibers increases lipolysis, and decreased sympathetic output leads to hypertrophy of gonadal WAT (19, 21).

Metabolic dysfunction in mGluR5$^{2L/2L:SF1\text{-}cre}$ females was associated with reduced intrinsic excitability, as well as altered excitatory and inhibitory synaptic transmission and a 43% reduction in firing rate in SF1 neurons. Notably, all of these physiological parameters were normal in SF1 neurons of mutant males, consistent with their intact metabolic profile. The diminished excitatory tone in SF1 neurons of naïve mGluR5$^{2L/2L:SF1\text{-}cre}$ females could be explained by the observed reduction in density of excitatory synapses onto these cells. The significant increase in inhibitory drive, for its part, results from increased inhibitory synaptic inputs and elevated levels of GAD67. Accordingly, levels of GAD67 mRNA in hypothalamic AgRP neurons were found to reliably predict levels of GABA release and GABAergic transmission (33).

Hypoactivity of SF1 neurons in mGluR5$^{2L/2L:SF1\text{-}cre}$ females likely contributes to their metabolic dysfunction, considering previous studies showing that chemogenetic activation of these

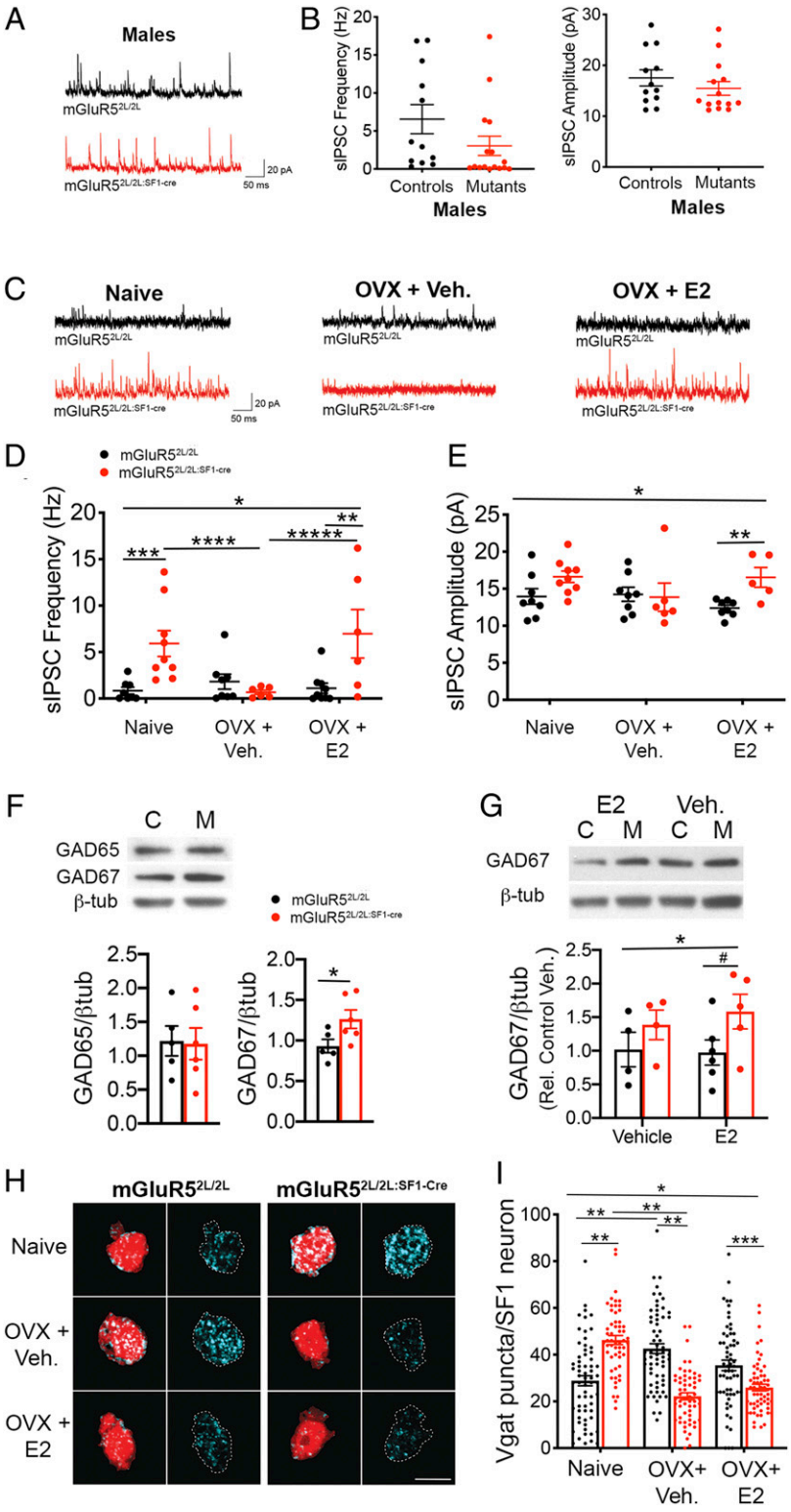

Fig. 7. Inhibitory neurotransmission in SF1 neurons is potentiated and paradoxically facilitated by estrogen in female mGluR5$^{2L/2L:SF1\text{-}cre}$ mice. (*A*) Representative sIPSC traces from SF1 neurons from male mGluR5$^{2L/2L}$ and mGluR5$^{2L/2L:SF1\text{-}cre}$ mice. (*B*) sIPSC frequency (Hz) and amplitude (pA) from SF1 neurons in mGluR5$^{2L/2L}$ (n = 8 cells, n = 2 animals) and mGluR5$^{2L/2L:SF1\text{-}cre}$ (n = 13 cells, n = 5 animals) males. (*C*) Representative sIPSC traces from SF1 neurons from naïve, OVX + vehicle, and OVX + E2 mGluR5$^{2L/2L}$ and mGluR5$^{2L/2L:SF1\text{-}cre}$ females. (*D*) sIPSC frequency (Hz) from naïve mGluR5$^{2L/2L}$ (n = 12 cells, n = 5 animals) and mGluR5$^{2L/2L:SF1\text{-}cre}$ (n = 11 cells, n = 4 animals) females, OVX mGluR5$^{2L/2L}$ (n = 9 cells, n = 3 animals) and mGluR5$^{2L/2L:SF1\text{-}cre}$ (n = 10 cells, n = 4 animals) females treated with vehicle, and OVX mGluR5$^{2L/2L}$ (n = 10 cells, n = 4 animals) and mGluR5$^{2L/2L:SF1\text{-}cre}$ (n = 10 cells, n = 3 animals) females treated with E2. Two-way ANOVA: genotype, P = 0.03; interaction of genotype and treatment, P = 0.008. Bonferroni's multiple comparisons test P values indicated. (*E*) sIPSC amplitude (pA) in SF1 neurons from naïve, OVX + vehicle, and OVX + E2 mGluR5$^{2L/2L}$ and mGluR5$^{2L/2L:SF1\text{-}cre}$ females. Two-way ANOVA: interaction of genotype and treatment, P = 0.05. Bonferroni's multiple comparisons test P values indicated. Data presented as mean ± SEM. (*F*) GAD65 and GAD67 expression in VMH normalized to β-tubulin content in naïve mGluR5$^{2L/2L}$ (n = 5) and mGluR5$^{2L/2L:SF1\text{-}cre}$ (n = 6) females. Student's t test, *P = 0.04. (*G*) GAD67 expression in VMH normalized to β-tubulin content in control ("C") mGluR5$^{2L/2L}$ (OVX + vehicle, n = 4; OVX + E2, n = 6) and mutant ("M") mGluR5$^{2L/2L:SF1\text{-}cre}$ (OVX + vehicle, n = 4; OVX + E2, n = 5) females. Two-way ANOVA: significant effect of genotype on GAD67 expression, P = 0.05. $^{\#}P$ = 0.1, Bonferroni's multiple comparisons test. (*H*) Representative immunolabeling of presynaptic vGAT^{+} (cyan) puncta onto SF1^{+} of naïve, OVX + vehicle, and OVX + E2 mGluR5$^{2L/2L}$ and mGluR5$^{2L/2L:SF1\text{-}cre}$ females. (*I*) Quantification of vGAT^{+} puncta onto SF1 neurons of mGluR5$^{2L/2L}$ and mGluR5$^{2L/2L:SF1\text{-}cre}$ females (n = 3 mice and n = 18 to 20 cells per animal). *Two-way ANOVA: genotype, P = 0.009; treatment, P = 0.001; interaction of genotype and treatment, P < 0.0001. Bonferroni's multiple comparisons test: **P < 0.0001; ***P = 0.007. Data presented as means ± SEM.

cells elevated peripheral insulin signaling and glucose mobilization (37). Furthermore, we show that neuronal activity in the VMH as marked by c-fos^{+} immunoreactivity was dramatically reduced in fasted mGluR5$^{2L/2L:SF1\text{-}Cre}$ females delivered a bolus of glucose. Finally, the finding that estrogen has opposite effects on both glucose tolerance and excitability of SF1 neurons in mutant females compared to controls also supports our model. We acknowledge that the lack of measurements of c-fos^{+} cells in fasted, vehicle-treated controls and mutants is a limitation of this study. However, a low density of c-fos^{+} cells (~25 to 30 per section) in the VMH of C57Bl6 mice fasted for 18 h and a rapid elevation in these cells (~50 to 55 cells per section) following 1 h of refeeding was reported previously (38).

Interestingly, previous studies showed that optogenetic inhibition of SF1 neurons or inhibition of glutamate release by those cells impaired the counterregulatory response to hypoglycemia

(39, 40). In contrast, our studies did not reveal any deficits in recovery from insulin-induced hypoglycemia. Another study showed that preventing glutamate release by SF1 neurons conferred resistance to diet-induced obesity and improved glycemic control in females but not in males (41). The collective studies illustrate the complexity of VMH metabolic circuits and how differences in outcomes might arise from the animal models used, that is, manipulating activity of the whole $SF1^+$ cell population versus a more discrete gene deletion that might affect a subpopulation of SF1 neurons. This is important to consider, acknowledging that there is functional heterogeneity within $SF1^+$ cells in the VMH (42). Additionally, whereas glutamate output clearly plays an important part in metabolic function, it is important to consider that other factors released by SF1 neurons may also play key roles.

The finding that every metabolic and electrophysiological parameter examined was affected in mutant $mGluR5^{2L/2L:SF1\text{-}cre}$ females but not males led us to investigate the involvement of sex hormones. Previous investigations indicated that estrogen signaling in the VMH contributes to sexual dimorphism in glucose balance control (43). Our work shows that mGluR5 depletion in VMH resulted in both loss of the normally beneficial effects of ERα and a gain of detrimental GPER1 function on glycemic control in females. The loss of ERα function is particularly relevant considering that metabolic effects of estrogen are attributed primarily to this receptor. Aberrant effects of E2 were also evident in our electrophysiological examination of SF1 neurons. Estrogen affected excitatory and inhibitory transmission in $mGluR5^{2L/2L:SF1\text{-}cre}$ compared to $mGluR5^{2L/2L}$ mice in a way that decreased and increased SF1 neuronal excitability, respectively. However, it is possible that estrogen receptors do not directly interact with mGluR5 but that their actions in other cells affect mGluR5-containing neurons in the VMH.

It is important to consider whether metabolic dysfunction in $mGluR5^{2L/2L:SF1\text{-}cre}$ females is related to developmental alterations rather than perturbation of adult functions of mGluR5 involving ERα. Indeed, expression of SF1 has been reported to be limited to the central and dmVMH, whereas that of ERα has been reported to be restricted to the vlVMH in the mature brain (24–26). Furthermore, SF1 is transiently expressed in neurons in the ventrolateral VMH that do not express this transcription factor in adulthood (24). Consistent with a role in adulthood, we found that SF1 neurons in central and dmVMH are estrogen-sensitive and that this hormone regulates the synaptic physiology and activity of those cells in mature animals in a mGluR5-dependent manner. For example, the density of inhibitory inputs and the firing rate of $SF1^+$ neurons in central and dmVMH of control $mGluR5^{2L/2L}$ females, which are effectively normal and do not have developmental confounds, were significantly influenced by levels of estradiol. Additionally, we and a study from the ABI detected $ERα^+$ cells in the dmVMH and $SF1^+$ cells in the vlVMH (28, 29). Importantly, our studies show that a significant number of cells in the adult VMH have triple colocalization of SF1, mGluR5, and ERα. These findings might be in conflict with other studies due to differences in sensitivity of the detection methods used. Our studies employed RNAscope technology, which is highly sensitive and can detect a single transcript per cell (27). Additionally, a recent study using the ERalpha-Zsgreen reporter mouse reported $ERα^+$ cells in the central and dmVMH and that about half of those cells were glucose-sensitive (44). In total, the data support an adult role of mGluR5 regulating metabolic function. Nonetheless, a limitation of our studies is that mGluR5 was depleted early in development. Therefore, we cannot completely rule out that developmental effects unrelated to adult functions of mGluR5 contribute to the phenotypes that we observed, and future studies should investigate the effect of depleting this glutamate receptor in the mature VMH.

A functional interaction of mGluR5 with GPER1, which is expressed throughout the VMH (45), has not been reported previously. It is possible that mGluR5 regulates GPER1 coupling to signaling pathways that differentially impact SF1 neuronal activity. Consistent with this idea, GPER1 is one of the rare receptors that can couple to both to Gαs and Gαi, enabling it to activate or inhibit selective signaling pathways depending on cellular context (46). Furthermore, it can both amplify or diminish estrogen signaling by other estrogen receptors (47). Finally, the localized expression of GPER1 to VMH (48) synapses suggests that it may influence neurotransmission in this region.

Why does mGluR5 depletion exclusively affect SF1 neuronal activity and metabolic function in females? One explanation is that mGluR5 critically modulates the effects of ERα and GPER1 and that function of those estrogen receptors in VMH neurons is requisite for metabolic health in females but not in males. In support, ERα depletion in SF1 neurons elicits metabolic disturbances only in females (7). Moreover, GPER1-knockout females but not males exhibit protection against glucose intolerance and hyperinsulinemia following chronic administration of a high-fat diet (49).

In summary, we report a sex-specific role of mGluR5 regulating firing rate, intrinsic excitability, and excitatory and inhibitory transmission in VMH SF1 neurons in female mice, facilitating glycemic control and lipid metabolism. Furthermore, we show that intact mGluR5 function in SF1 neurons is requisite for estrogen to achieve its positive effects on VMH neuronal activity and glucose homeostasis. These investigations inform mechanisms underlying the protective effects of estrogen against metabolic disease and the higher risk of diabetes in postmenopausal women.

Methods

Animals. All procedures were approved by the institutional animal care and use committee at Tufts University and conducted in accordance with the National Institutes of Health Guide for Care and Use of Laboratory Animals guidelines. $BDNF^{2L/2L:Ck\text{-}cre}$ mice were generated as previously described (9). Mice with specific mGluR5 depletion in SF1-positive neurons were generated by crossing floxed mGluR5 mice with SF1-Cre transgenic mice obtained from the Jackson Laboratory (stock no. 012462), and they were in a C57BL/6J-129 hybrid background. For the electrophysiology experiments, mice containing the floxed mGluR5 and SF1-cre alleles were crossed to mice with cre-dependent expression of tdTomato (stock no. 007914) obtained from the Jackson Laboratory.

Western Blot Analysis. To isolate VMH from acute brain tissue, mice (12 to 16 wk old) were anesthetized using isoflurane, then decapitated. Brains were removed and mounted onto a Leica VT1000S vibrating microtome in cold 1× PBS. An 800-μm coronal section from bregma −1.25 mm to −2.05 mm containing the VMH was extracted. The VMH was then microdissected from the sections using a dissecting scope and flash-frozen. Protein was extracted, and Western blot analysis was performed using standard methods (12, 50). Blot images were acquired using a Fujifilm LAS-4000 image reader, and densitometry was performed using Quantity One analysis software (BioRad). The following primary antibodies were used: anti-mGluR5 (1:1,000; Millipore no. AB5675), anti-ERα (1:1,000; Cell Signaling Technology no. 8644), anti-ERβ (1:500; Abcam no. ab3576), anti-GPR30 (1:1,000; Thermo Fisher no. PA5-77396), anti-GAD65 (1:2,000; Sigma no. G1166), anti-GAD67 (1:20,000; Millipore no. MAB5406), anti-AMPA1 (1:1,000; Cell Signaling Technology no. D4N9V), anti-GLUN1 (1,000; Cell Signaling Technology no. D65B7), anti-$GABA_Aγ$ (1:2,000; PhosphoSolutions no. 830-GG2), and anti–β-tubulin (1:10,000; Sigma no. T4026).

Food Intake and Body Weight Measurements. Mice were individually housed with unrestricted access to water and a premeasured amount of food. Weekly body weight and food intake measurements were taken beginning at 6 wk of age at the same time of day. Animals were fed a standard chow diet (SC) with 18.6% protein, 6.2% fat, and a caloric content of 3.1 kcal/g (Envigo 2918) or a high-fat diet (HFD) with 45% kcal fat, 20% kcal protein, 35% kcal carbohydrate, and a caloric content of 4.7 kcal/g (Research Diets D12451).

Locomotor Activity. Mice (8 to 12 wk of age) were individually housed in their home cages (standard 15 × 24-cm plastic cages) surrounded by the Smart

Frame Activity System photobeam frame. Locomotor activity, as measured by beam breaks, was recorded continuously using MotorMontitor software (Hamilton/Kinder).

Body Temperature Measurements. Core body temperature was measured in mice (8 to 12 wk of age) using the MicroTherma 2T Hand Held Thermometer (Braintree Scientific) fitted with a mouse rectal probe, stabilized for >5 s.

Glucose and Insulin Tolerance Tests. Mice were fasted for 16 h, and tail blood glucose values were measured using a Freestyle Blood Glucose Monitoring System (Abbott Diabetes Care). Following a baseline (0) measurement, 1.5 g/kg of D-glucose was administered intraperitoneally (i.p.). For the insulin tolerance test (ITT), animals were fasted for 6 h prior to the baseline (0) blood glucose measurement. Mice were then administered 0.85 U/kg insulin (Human-R Insulin U100; Lily) via i.p. injection.

Immunofluorescence. Mice (8 to 12 wk old) were anesthetized and perfused with cold saline followed by 4% paraformaldehyde (PFA). Brains were removed, postfixed in 4% PFA for 4 h at 4 °C, and cryoprotected in a 30% sucrose solution. Coronal sections (30 μm thick) were incubated for 16 h at 4 °C with the following primary antibodies: anti-mGluR5 (1:250; Alamone AGC-007), anti-Nr5a1(Ad4BP/SF1) (1:250; TransGenic 1B1510), anti-Nr5a1(SF1) (1:250; Thermo Fisher 434200), anti-NeuN (1:1,000; Abcam 177487), anti-vGlut2 (1:500; Millipore AB2251-I), and anti-VGAT (1:500; SYSY 131004). Sections were then incubated with the appropriate secondary antibodies. For the c-fos immunofluorescence experiments, control and mutant females fasted for 16 h received a bolus of glucose (1.5 g/kg of D-glucose) via i.p. injection and were euthanized 30 min later. VMH-containing sections were incubated overnight at 4 °C with anti–c-fos (1:200; Santa Cruz SC-52-G) followed by a 1-h RT incubation with secondary antibody. A Nikon A1R confocal microscope was used to capture images of all brain sections.

Quantification of Excitatory and Inhibitory Synapses. To quantify excitatory and inhibitory inputs onto SF1 neurons, sections were coimmunolabeled with anti-NeuN, SF1, and vGlut2 or vGAT. Ten-micrometer *z*-stack images were captured at 64× on a Nikon A1R microscope. Three-dimensional reconstructions of SF1 neurons were generated using the Surfaces tool in Imaris Image Analysis Software. An SF1-positive nuclear signal was used to identify SF1-positive neurons, and 3D reconstructions were generated using the NeuN stain, which fills the entire cell body. vGlut2 or vGAT puncta within the volume of each SF1 neuron reconstruction were isolated and exported into ImageJ for quantification.

In Situ Hybridization/RNAscope. Brains from wild type C57Bl6 female and male mice (8 to 10 wk of age) were processed as for the immunofluorescence studies. Sections (12 μm thick) were processed using the RNAscope fluorescent multiplex reagent kit (ACD) and following the manufacturer's recommendations. The following probes were used: Mm-Grm5-C2 (mGluR5), Mm-Nr5a1 (SF1), Probe Mm-Esr1-C3 (ERα), Mm-Esr2-C3 (ERβ), and Mm-Gper1-C3 (GPER-1; ACD). Images of VMH sections subjected to RNAscope analysis were acquired by confocal microscopy (Nikon A1R) using a 40× oil immersion objective lens. Colocalization of transcript signals was analyzed using a custom CellProfiler pipeline (https://cellprofiler.org/) created to count the number of cells with colocalization of SF-1, mGluR5, and estrogen receptor transcript signals. Cells with detection of five or more dots (transcripts) were considered positive for a marker.

Electrophysiology. Mice (8 to 12 wk of age) were anesthetized by isoflurane inhalation and decapitated, and brains were extracted. Coronal sections (300 μm) were prepared using a Leica VT1000S microtome and maintained in oxygenated (95% O_2/5% CO_2) aCSF containing 26 mM $NaHCO_3$, 126 mM NaCl, 2.5 mM KCl, 1.25 mM NaH_2PO_4, 1 mM $MgSO_4$, 2 mM $CaCl_2$, and 10 mM D-glucose at 32 °C for 1 h prior to recording. Whole-cell recordings were made in $SF1^+$ neurons in central and dmVMH at 32 °C using the Nikon Eclipse FN1 microscope, a MultiClamp 700B amplifier (Axon Instruments), Digidata 1440A Digitizer (Axon Instruments), and pClamp program software (Axon Instruments) and sampled at 10 kHz. For voltage clamp recordings, a cesium-based internal solution was used containing 120 mM D-gluconic acid, 10 mM Hepes, 0.5 mM $CaCl_2$, 20 mM TEA-Cl, 120 mM CsOH, 10 mM EGTA, 2 mM ATP, and 0.3 mM GTP, with a final osmolality between 295 to 300 mOsmol. For current clamp recordings, a potassium-based internal solution was used containing 135 mM $KMeSO_3$, 3 mM KCl, 10 mM Hepes, 1 mM EGTA, 0.1 mM $CaCl_2$, 8 mM Na_2-phosphocreatine, 4 mM ATP, and 0.3 mM GTP with a final osmolality of 295 mOsmol.

sEPSC measurements were performed in slices submerged in aCSF containing 10 μM SR 95531 (Tocris). sIPSC measurements were performed in slices submerged in aCSF, and 10 μM SR 95531 (Tocris) was washed onto slices after completion of the experiment to ensure currents were GABA-driven. sEPSC and sIPSC recordings were analyzed using Mini Analysis Program (Synaptosoft). Neurons were current-clamped with 0 pA current injected for spike frequency recordings and membrane potential measurements. Membrane potentials were corrected for an ∼8-mV liquid junction potential. The number of action potentials generated in response to a series of 500-ms current injections from 20 to 200 pA in 20-pA steps were measured in the current-clamp configuration. Data analysis was performed using Clampfit (Axon Instruments).

Ovariectomy and Silastic Capsule Implantation. $mGluR5^{2L/2L:SF1\text{-}cre}$ and $mGluR5^{2L/2L}$ females (8 to 12 wk old) were anesthetized with ketamine (100 mg/kg) and xylazine (10 mg/kg), and bilateral ovariectomies were performed, followed by s.c. implants of silastic capsules filled with 17β-estradiol (E2, 2 μg/μL), the estrogen receptor α agonist 4,4′,4′′-(4-Propyl-[1*H*]-pyrazole-1,3,5-triyl)*Tris*-phenol (PPT, 2 μg/μL; Tocris no. 1426), estrogen receptor β agonist diarylpropionitrile (DPN, 2 μg/μL; Tocris no. 1494), GPER1 receptor agonist G-1 (10 μg/μL; Tocris, no. 3577), or vehicle. Body weights were measured weekly, and, after 5 wk, mice were subjected to a GTT.

Tissue Measurements. Triglyceride concentrations in liver, white adipose tissue, and serum samples were determined by the Vanderbilt Hormone Assay and Analytical Services Core. Norepinephrine content in serum samples was analyzed using HPLC methods by the Neurochemistry Core Laboratory at the Vanderbilt Brain Institute. Serum insulin (Insulin ELISA kit; Mercodia) was measured following the manufacturer's instructions.

Histology of Adipose Tissue. Perigonadal white adipose tissue samples were extracted and fixed in 10% neutral buffered formalin. Paraffin embedding and H&E staining was performed by the Tufts Histology Core. Images acquired on the Zeiss Axioplan 2 microscope at 10× magnification were captured with a Retiga 1300B camera. Adipocyte size was measured using the ImageJ open-source software plugin Adiposoft.

Statistical Analysis. GraphPad Prism analytical software was used to perform the statistical analysis. Repeated-measures ANOVA, using Bonferroni's method to adjust for multiple comparisons, was performed to analyze weekly body weight measurements as well as the time course data for the glucose and insulin tolerance tests. Two-way ANOVAs were used to analyze locomotor activity, thermoregulation, insulin levels, triglyceride content, serum norepinephrine, area under the curve for glucose and insulin tolerance tests, and excitatory and inhibitory synapse density. Three-way ANOVAs were used to analyze data from GTTs in OVX females treated with estrogen receptor agonists. Student's unpaired *t* tests were performed to analyze comparisons of two groups including mGluR5 protein expression, food intake, adipocyte size, and protein expression of ERα, ERβ, and GPER1. Comparisons were determined to be statistically significant when $P < 0.05$. All values are depicted as mean ± SEM.

Data Availability. All relevant data are included in the main text and *SI Appendix*.

ACKNOWLEDGMENTS. These studies were supported by NIH/NIDDK Grants to M.R. (DK073311 and DK113445) and D.A. (F31 DK118789) and the core facilities at the Tufts Center for Neuroscience Research and the Vanderbilt lipid core facility, supported by Grant DK59637 for facilitating these studies.

1. B. M. King, The rise, fall, and resurrection of the ventromedial hypothalamus in the regulation of feeding behavior and body weight. *Physiol. Behav.* **87**, 221–244 (2006).
2. S. Kühnemann, T. J. Brown, R. B. Hochberg, N. J. MacLusky, Sex differences in the development of estrogen receptors in the rat brain. *Horm. Behav.* **28**, 483–491 (1994).
3. V. H. Routh, Glucose sensing neurons in the ventromedial hypothalamus. *Sensors (Basel)* **10**, 9002–9025 (2010).
4. T. Klöckener *et al*., High-fat feeding promotes obesity via insulin receptor/PI3K-dependent inhibition of SF-1 VMH neurons. *Nat. Neurosci.* **14**, 911–918 (2011).
5. R. Zhang *et al*., Selective inactivation of Socs3 in SF1 neurons improves glucose homeostasis without affecting body weight. *Endocrinology* **149**, 5654–5661 (2008).
6. J. Cao, H. B. Patisaul, Sexually dimorphic expression of hypothalamic estrogen receptors α and β and Kiss1 in neonatal male and female rats. *J. Comp. Neurol.* **519**, 2954–2977 (2011).

7. Y. Xu *et al*., Distinct hypothalamic neurons mediate estrogenic effects on energy homeostasis and reproduction. *Cell Metab.* **14**, 453–465 (2011).
8. A. Patapoutian, L. F. Reichardt, Trk receptors: Mediators of neurotrophin action. *Curr. Opin. Neurobiol.* **11**, 272–280 (2001).
9. M. Rios *et al*., Conditional deletion of brain-derived neurotrophic factor in the postnatal brain leads to obesity and hyperactivity. *Mol. Endocrinol.* **15**, 1748–1757 (2001).
10. T. J. Unger, G. A. Calderon, L. C. Bradley, M. Sena-Esteves, M. Rios, Selective deletion of Bdnf in the ventromedial and dorsomedial hypothalamus of adult mice results in hyperphagic behavior and obesity. *J. Neurosci.* **27**, 14265–14274 (2007).
11. B. Xu *et al*., Brain-derived neurotrophic factor regulates energy balance downstream of melanocortin-4 receptor. *Nat. Neurosci.* **6**, 736–742 (2003).
12. J. W. Cordeira *et al*., Hypothalamic dysfunction of the thrombospondin receptor $\alpha2\delta$-1 underlies the overeating and obesity triggered by brain-derived neurotrophic factor deficiency. *J. Neurosci.* **34**, 554–565 (2014).
13. E. K. Speliotes *et al*.; MAGIC; Procardis Consortium, Association analyses of 249,796 individuals reveal 18 new loci associated with body mass index. *Nat. Genet.* **42**, 937–948 (2010).
14. E. Hermans, R. A. Challiss, Structural, signalling and regulatory properties of the group I metabotropic glutamate receptors: prototypic family C G-protein-coupled receptors. *Biochem. J.* **359**, 465–484 (2001).
15. M. T. Sepulveda-Orengo, A. V. Lopez, O. Soler-Cedeño, J. T. Porter, Fear extinction induces mGluR5-mediated synaptic and intrinsic plasticity in infralimbic neurons. *J. Neurosci.* **33**, 7184–7193 (2013).
16. A. N. van den Pol, C. Romano, P. Ghosh, Metabotropic glutamate receptor mGluR5 subcellular distribution and developmental expression in hypothalamus. *J. Comp. Neurol.* **362**, 134–150 (1995).
17. J. Gibon, P. A. Barker, P. Séguéla, Opposing presynaptic roles of BDNF and ProBDNF in the regulation of persistent activity in the entorhinal cortex. *Mol. Brain* **9**, 23 (2016).
18. Z. Song, B. E. Levin, J. J. McArdle, N. Bakhos, V. H. Routh, Convergence of pre- and postsynaptic influences on glucosensing neurons in the ventromedial hypothalamic nucleus. *Diabetes* **50**, 2673–2681 (2001).
19. M. Ruffin, S. Nicolaidis, Electrical stimulation of the ventromedial hypothalamus enhances both fat utilization and metabolic rate that precede and parallel the inhibition of feeding behavior. *Brain Res.* **846**, 23–29 (1999).
20. D. Lindberg, P. Chen, C. Li, Conditional viral tracing reveals that steroidogenic factor 1-positive neurons of the dorsomedial subdivision of the ventromedial hypothalamus project to autonomic centers of the hypothalamus and hindbrain. *J. Comp. Neurol.* **521**, 3167–3190 (2013).
21. W. Zeng *et al*., Sympathetic neuro-adipose connections mediate leptin-driven lipolysis. *Cell* **163**, 84–94 (2015).
22. D. Grove-Strawser, M. I. Boulware, P. G. Mermelstein, Membrane estrogen receptors activate the metabotropic glutamate receptors mGluR5 and mGluR3 to bidirectionally regulate CREB phosphorylation in female rat striatal neurons. *Neuroscience* **170**, 1045–1055 (2010).
23. B. M. Peterson, P. G. Mermelstein, R. L. Meisel, Estradiol mediates dendritic spine plasticity in the nucleus accumbens core through activation of mGluR5. *Brain Struct. Funct.* **220**, 2415–2422 (2015).
24. C. C. Cheung, D. M. Kurrasch, J. K. Liang, H. A. Ingraham, Genetic labeling of steroidogenic factor-1 (SF-1) neurons in mice reveals ventromedial nucleus of the hypothalamus (VMH) circuitry beginning at neurogenesis and development of a separate non-SF-1 neuronal cluster in the ventrolateral VMH. *J. Comp. Neurol.* **521**, 1268–1288 (2013).
25. S. M. Correa *et al*., An estrogen-responsive module in the ventromedial hypothalamus selectively drives sex-specific activity in females. *Cell Rep.* **10**, 62–74 (2015).
26. M. Koch, Effects of treatment with estradiol and parental experience on the number and distribution of estrogen-binding neurons in the ovariectomized mouse brain. *Neuroendocrinology* **51**, 505–514 (1990).
27. F. Wang *et al*., RNAscope: A novel in situ RNA analysis platform for formalin-fixed, paraffin-embedded tissues. *J. Mol. Diagn.* **14**, 22–29 (2012).
28. Allen Institute. Allen Brain Atlas Experiment 734. https://mouse.brain-map.org/experiment/show/734. Accessed 29 April 2020.
29. Allen Institute. Allen Brain Atlas Experiment 79591677. https://mouse.brain-map.org/experiment/show/79591677. Accessed 29 April 2020.
30. S. Musatov *et al*., Silencing of estrogen receptor alpha in the ventromedial nucleus of hypothalamus leads to metabolic syndrome. *Proc. Natl. Acad. Sci. U.S.A.* **104**, 2501–2506 (2007).
31. C. Ohlsson *et al*., Obesity and disturbed lipoprotein profile in estrogen receptor-alpha-deficient male mice. *Biochem. Biophys. Res. Commun.* **278**, 640–645 (2000).
32. A. Naaz *et al*., Effect of ovariectomy on adipose tissue of mice in the absence of estrogen receptor alpha (ERalpha): A potential role for estrogen receptor beta (ERbeta). *Horm. Metab. Res.* **34**, 758–763 (2002).
33. M. S. Dicken, A. R. Hughes, S. T. Hentges, Gad1 mRNA as a reliable indicator of altered GABA release from orexigenic neurons in the hypothalamus. *Eur. J. Neurosci.* **42**, 2644–2653 (2015).
34. C. G. Lau, V. N. Murthy, Activity-dependent regulation of inhibition via GAD67. *J. Neurosci.* **32**, 8521–8531 (2012).
35. T. Shimazu, M. Sudo, Y. Minokoshi, A. Takahashi, Role of the hypothalamus in insulin-independent glucose uptake in peripheral tissues. *Brain Res. Bull.* **27**, 501–504 (1991).
36. M. Sudo, Y. Minokoshi, T. Shimazu, Ventromedial hypothalamic stimulation enhances peripheral glucose uptake in anesthetized rats. *Am. J. Physiol.* **261**, E298–E303 (1991).
37. E. A. Coutinho *et al*., Activation of SF1 neurons in the ventromedial hypothalamus by DREADD technology increases insulin sensitivity in peripheral tissues. *Diabetes* **66**, 2372–2386 (2017).
38. Q. Wu *et al*., The temporal pattern of cfos activation in hypothalamic, cortical, and brainstem nuclei in response to fasting and refeeding in male mice. *Endocrinology* **155**, 840–853 (2014).
39. T. H. Meek *et al*., Functional identification of a neurocircuit regulating blood glucose. *Proc. Natl. Acad. Sci. U.S.A.* **113**, E2073–E2082 (2016).
40. Q. Tong *et al*., Synaptic glutamate release by ventromedial hypothalamic neurons is part of the neurocircuitry that prevents hypoglycemia. *Cell Metab.* **5**, 383–393 (2007).
41. C. C. Cheung *et al*., Sex-dependent changes in metabolism and behavior, as well as reduced anxiety after eliminating ventromedial hypothalamus excitatory output. *Mol. Metab.* **4**, 857–866 (2015).
42. J. W. Sohn *et al*., Leptin and insulin engage specific PI3K subunits in hypothalamic SF1 neurons. *Mol. Metab.* **5**, 669–679 (2016).
43. A. M. Santiago, D. J. Clegg, V. H. Routh, Estrogens modulate ventrolateral ventromedial hypothalamic glucose-inhibited neurons. *Mol. Metab.* **5**, 823–833 (2016).
44. Y. He *et al*., Estrogen receptor-α expressing neurons in the ventrolateral VMH regulate glucose balance. *Nat. Commun.* **11**, 2165 (2020).
45. E. Brailoiu *et al*., Distribution and characterization of estrogen receptor G protein-coupled receptor 30 in the rat central nervous system. *J. Endocrinol.* **193**, 311–321 (2007).
46. M. M. Hadjimarkou, N. Vasudevan, GPER1/GPR30 in the brain: Crosstalk with classical estrogen receptors and implications for behavior. *J. Steroid Biochem. Mol. Biol.* **176**, 57–64 (2018).
47. S. N. Romano, D. A. Gorelick, Crosstalk between nuclear and G protein-coupled estrogen receptors. *Gen. Comp. Endocrinol.* **261**, 190–197 (2018).
48. G. G. Hazell *et al*., Localisation of GPR30, a novel G protein-coupled oestrogen receptor, suggests multiple functions in rodent brain and peripheral tissues. *J. Endocrinol.* **202**, 223–236 (2009).
49. A. Wang *et al*., GPR30 regulates diet-induced adiposity in female mice and adipogenesis in vitro. *Sci. Rep.* **6**, 34302 (2016).
50. J. A. Felsted *et al*., Alpha2delta-1 in $SF1^{+}$ neurons of the ventromedial hypothalamus is an essential regulator of glucose and lipid homeostasis. *Cell Rep.* **21**, 2737–2747 (2017).